

DOCUMENT ROOM ~~DOCUMENT~~ ROOM 36-412  
RESEARCH LABORATORY OF ELECTRONICS  
MASSACHUSETTS INSTITUTE OF TECHNOLOGY

*Copy 3*

## UNDIRECTIONAL PARAMAGNETIC AMPLIFIER DESIGN

M. W. P. STRANDBERG

TECHNICAL REPORT 363

JUNE 26, 1959

*See Copy Only*

RESEARCH LABORATORY OF ELECTRONICS  
MASSACHUSETTS INSTITUTE OF TECHNOLOGY  
CAMBRIDGE, MASSACHUSETTS

The Research Laboratory of Electronics is an interdepartmental laboratory of the Department of Electrical Engineering and the Department of Physics. The research reported in this document was made possible in part by support extended the Massachusetts Institute of Technology, Research Laboratory of Electronics, jointly by the U.S. Army (Signal Corps), the U.S. Navy (Office of Naval Research), and the U.S. Air Force (Office of Scientific Research, Air Research and Development Command), under Signal Corps Contract DA36-039-sc-78108, Department of the Army Task 3-99-20-001 and Project 3-99-00-000.

# Unidirectional Paramagnetic Amplifier Design\*

M. W. P. STRANDBERG†, FELLOW, IRE

**Summary**—The radio-frequency parameters and the quantum-mechanical parameters entering into the design of paramagnetic quantum-mechanical amplifiers are described and discussed. The physical and electrical limitations on such parameters as gain-bandwidth product, gain stability, and nonreciprocity are described analytically and with design curves. Two realizations of nonreciprocal amplifiers are described and discussed. In particular, operation of a nonreciprocal amplifier at 9 kmc is described. Explanations for the observed properties of previously reported amplifiers are given, and the steps necessary to achieve high gain-bandwidth product and nonreciprocity with paramagnetic amplifiers are described.

## INTRODUCTION

OF THE MANY desirable characteristics of a solid-state amplifier, such as large gain-bandwidth product, low noise figure, and tunability,<sup>1</sup> one important quality is a unidirectional and nonreciprocal amplification characteristic. Although it has been pointed out<sup>1</sup> that these amplification characteristics are achievable by using circularly-polarized electromagnetic fields and the inherent Faraday effect of paramagnetic systems, little interest in development of

amplifiers along these lines is apparent. This is difficult to understand because, for example, the application of paramagnetic amplifiers to *L*-band radioastronomy is hampered by the lack of a lossless *L*-band circulator. Furthermore, other methods of obtaining unidirectional gain—for example, through the use of a circulator (nonreciprocal) or through the use of a negative-resistance bridge—are incomparably more difficult to engineer for acceptable performance than is a circular-polarization amplifier. Probably the only other reason for the absence of interest in a circular-polarization amplifier arises from the fact that a concrete and detailed design does not exist. This paper offers a simple and easily realizable design for a circularly-polarized cavity amplifier. The basic idea upon which the amplifier rests is quite simple. It is that a two-port RF system can be made to absorb or to emit, coherently, energy in a unidirectional fashion if the RF fields comprising the system are resolvable into two orthogonal field systems. This system can also have nonreciprocal gain if the matter in which the fields exist exhibits a Faraday effect and the orthogonal modes are positive and negative circularly-polarized fields. The system need not exhibit a pure Faraday effect, however, and still have a nonreciprocity of gain which is sufficient to stabilize the amplifier against gain-fluctuation arising from variation of the reflection coefficient of the input or output ports.

## AMPLIFIER STRUCTURE

This discussion will be restricted to a regenerative or cavity paramagnetic amplifier. This is not a severe restriction; ample gain-bandwidth product is available from such structures, and they can be cascaded by any number of means to form an amplifying structure with over-all gain and bandwidth characteristics equal to those envisaged by present slow-wave structures. Whether one calls such a structure a cascade of low-loaded *Q* resonant systems or a slow-wave structure is a matter of semantics rather than of engineering. The relationship between the *Q* of the structure, the gain in decibels per free-space wavelength *G'*, and the wave-slowing factor *s*, the ratio of the group velocity *v<sub>g</sub>*, of the structure to the velocity of light *c* is,

$$Q = \frac{20\pi s \log(e)}{G'} \quad (1)$$

The type of structure to be used is obviously dictated by the gain and bandwidth requirements for any particular application. For example, in the hydrogen-line radioastronomy studies at 1420 mc, a bandwidth of 300 mc with a gain of 20 db would be sufficient; but for ther-

\* Original manuscript received by the IRE, June 26, 1959; revised manuscript received, January 12, 1960. This work was supported in part by the U. S. Army Signal Engineering Laboratories and in part by the U. S. Army (Signal Corps), the U. S. Air Force (Office of Scientific Research, Air Research and Development Command), and the U. S. Navy (Office of Naval Research).

† Res. Lab. of Electronics, Mass. Inst. Tech., Cambridge, Mass.

<sup>1</sup> M. W. P. Strandberg, "Quantum-mechanical amplifiers," *Proc. IRE*, vol. 45, pp. 92-93; January, 1957. As a matter of historical accuracy, it is necessary to point out that many of these ideas were developed in collaboration with H. R. Johnson in the summer of 1955. Pioneering work on ammonia beam experiments (see H. R. Johnson and M. W. P. Strandberg, "Beam system for reduction of Doppler broadening of a microwave absorption line," *Phys. Rev.*, vol. 85, pp. 503-504; February 1, 1952) had indicated the limitations on the use of ammonia beam masers as practical amplifiers. Discussions, which were held in Cambridge, Massachusetts, and in Culver City, California, established a firm scientific basis for confidence in the ultimate and tremendous usefulness of solid-state amplifiers. Simple though it sounds, the novel idea at that time was that paramagnetic materials presented the means by which one could make a practical quantum-mechanical amplifier with large gain-bandwidth product, low noise figure, tunability, and large dynamic range. In 1955, the state of development of quantum-mechanical amplifiers showed a lack of ability to achieve all of these qualities rather than lack of confidence in being able to build amplifiers, since all of the methods for obtaining negative resistance in gases and solids that are known today had been disclosed (and some demonstrated) at that time. General design problems were given further consideration by the writer and were discussed with various people. Some of these ideas were presented at a Physics Department Colloquium at M.I.T., in May, 1956. These discussions inspired interest in many quarters in most of the elements of paramagnetic-amplifier design and use, the outstanding exception being the realization of a circular-polarization cavity amplifier. A proper understanding of the noise figure of quantum-mechanical amplifiers was certainly not available before the analysis made by the writer and others in 1956 and, furthermore, the proper application of this theory in terms of observed circuit parameters was not well understood even after that. The actual translation of theory into application to actual devices is always difficult; this paper is merely intended, again, as a translation of theory into a concrete device. Cf. M. W. P. Strandberg, "Inherent noise of quantum-mechanical amplifiers," *Phys. Rev.*, vol. 106, pp. 617-620; May 15, 1957.

mal-source studies one would like to have a bandwidth of the order of the operating frequency and a gain of 20 db. For radar or communications applications, one would possibly have requirements for modest bandwidth of the order of a few tens of megacycles with gains of the order of 30 db. In some work there is also a requirement for high stability of gain of the device with changes in operating conditions. For example, in broadband radioastronomy, the thermal radiation is integrated in time in order to improve the sensitivity of the device. Here the requirement for the gain stability is high and has a high priority.

The traveling-wave amplifier has an exponential increase of gain with length as follows:

$$P_{\text{out}} = e^{\gamma l} P_{\text{in}} = G P_{\text{in}} \quad (2)$$

where

$$\gamma = \frac{8\pi^2 f \eta}{v_g} \text{Im}(\chi). \quad (3)$$

Here  $f$  is the wave frequency,  $\eta$  is the filling factor, and a single resonant term in the complex susceptibility is<sup>2</sup>

$$\chi = -\chi_0 \frac{f}{(f - f_0) + i \frac{B_x}{2}} \quad (4)$$

$$|r|^2 = G = \frac{16\overline{\Delta f^4} + 4\overline{\Delta f^2} \left[ B_e^2 \left(1 - \frac{Q_e}{Q_0}\right)^2 + B_x^2 - 2 \frac{Q_e}{Q_{x0}} B_e B_x \right] + B_e^2 B_x^2 \left(1 - \frac{Q_e}{Q_0} - \frac{Q_e}{Q_{x0}}\right)^2}{16\overline{\Delta f^4} + 4\overline{\Delta f^2} \left[ B_e^2 \left(1 + \frac{Q_e}{Q_0}\right)^2 + B_x^2 - 2 \frac{Q_e}{Q_{x0}} B_e B_x \right] + B_e^2 B_x^2 \left(1 + \frac{Q_e}{Q_0} + \frac{Q_e}{Q_{x0}}\right)^2} \quad (10)$$

with  $B_x$  the paramagnetic resonant linewidth. The gain thus exponentially follows the frequency variation of the susceptibility of the paramagnetic material both through the imaginary part of the susceptibility directly and through the real part of the susceptibility in its influence on the group velocity. If we neglect the latter effect, the 3-db bandwidth of a traveling-wave amplifier with a gain  $G$ , in decibels, is

$$B = B_x \left( \frac{3}{G_{\text{db}} - 3} \right)^{1/2}. \quad (5)$$

A similar expression can be derived for a single regenerative cavity. Previously, the amplifiers envisaged were of sufficiently narrow bandwidth that the frequency variation of the susceptibility could be neglected. This is not true in general. The introduction of the frequency dependence of the complex susceptibility for the paramagnetic material modifies the magnetic  $Q$ , so that it has a frequency dependence that is the reciprocal of the frequency dependence of the susceptibility

$$Q_x \rightarrow Q_{x0} \left( 1 + i \frac{2(f - f_0)}{B_x} \right) = (4\pi\chi\eta)^{-1}. \quad (6)$$

If a cavity containing this complex susceptibility terminates a transmission line having an admittance  $Y_0$ , it represents a load admittance,  $Y = g + ib$ , which is conventionally described in terms of the cavity unloaded  $Q$ ,  $Q_0$ , the magnetic  $Q$ ,  $Q_x$ , the coupling  $Q$ ,  $Q_e$ , and the frequency as:

$$\frac{g}{Y_0} = \frac{Q_e}{Q_x} + \frac{Q_e}{Q_0} \quad (7)$$

$$\frac{b}{Y_0} = 2Q_e \frac{(f - f_0)}{f_0} \equiv \frac{2\Delta f}{B_e}. \quad (8)$$

Then the reflection coefficient (or voltage gain) is:

$$r = \frac{Y_0 - Y}{Y_0 + Y} = \frac{\left(1 - \frac{Q_e}{Q_0} - i \frac{2\Delta f}{B_e}\right) \left(1 + i \frac{2\Delta f}{B_x}\right) - \frac{Q_e}{Q_{x0}}}{\left(1 + \frac{Q_e}{Q_0} + i \frac{2\Delta f}{B_e}\right) \left(1 + i \frac{2\Delta f}{B_x}\right) + \frac{Q_e}{Q_{x0}}} \quad (9)$$

The bandwidth,  $B$ , of a single-tuned stage is defined as the frequency width between the points at which the magnitude of the reflection coefficient squared is reduced to half of its value at resonance.

Therefore,

$$B^2 = \frac{1}{2} \left[ \left\{ \left[ 1 + \left( \frac{Q_e}{Q_0} \right)^2 \right] B_e^2 + B_x^2 - 2 \frac{Q_e}{Q_{x0}} B_e B_x \right. \right. \\ \left. \left. - 4 \frac{Q_e}{Q_0} B_e^2 \frac{3 + 2 \left( \frac{Q_e}{Q_0} + \frac{Q_e}{Q_{x0}} \right) + 3 \left( \frac{Q_e}{Q_0} + \frac{Q_e}{Q_{x0}} \right)^2}{1 + 6 \left( \frac{Q_e}{Q_0} + \frac{Q_e}{Q_{x0}} \right) + \left( \frac{Q_e}{Q_0} + \frac{Q_e}{Q_{x0}} \right)^2} \right\} \right. \\ \left. - \frac{4 B_e B_x \left( 1 - \left( \frac{Q_e}{Q_0} + \frac{Q_e}{Q_{x0}} \right)^2 \right)^2}{1 + 6 \left( \frac{Q_e}{Q_0} + \frac{Q_e}{Q_{x0}} \right) + \left( \frac{Q_e}{Q_0} + \frac{Q_e}{Q_{x0}} \right)^2} \right]^{1/2} \\ - \frac{1}{2} \left\{ \left[ 1 + \left( \frac{Q_e}{Q_0} \right)^2 \right] B_e^2 + B_x^2 - 2 \frac{Q_e}{Q_{x0}} B_e B_x \right. \\ \left. - 4 \frac{Q_e}{Q_0} B_e^2 \frac{3 + 2 \left( \frac{Q_e}{Q_0} + \frac{Q_e}{Q_{x0}} \right) + 3 \left( \frac{Q_e}{Q_0} + \frac{Q_e}{Q_{x0}} \right)^2}{1 + 6 \left( \frac{Q_e}{Q_0} + \frac{Q_e}{Q_{x0}} \right) + \left( \frac{Q_e}{Q_0} + \frac{Q_e}{Q_{x0}} \right)^2} \right\}. \quad (11)$$

<sup>2</sup> M. W. P. Strandberg, "Microwave Spectroscopy," Methuen and Company, Ltd., London, p. 70; 1954.

For large gain, the gain-bandwidth product can be reduced to

$$\sqrt{GB} \approx \frac{2}{\frac{1}{B_x} + \frac{Q_{x0}}{f_0}} \quad (12)$$

Care must be exercised in using expressions (5) and (12) for  $B$ ; for gains less than 3 db, a 3-db point does not exist.

If a series of these regenerative cavities is coupled in cascade, the gains of each stage will multiply and the frequency dependence of the gains will also multiply. The frequency dependence of the reflection coefficient may be crudely approximated by a curve of the form

$$|r|^2 = [1 + b^2]^{-1} |r|_{\max}^2. \quad (13)$$

In this case one may show that the net gain-bandwidth product for  $N$  synchronously-tuned cascaded cavities, each having a gain-bandwidth product of  $B_1$ , is given as

$$G^{1/(2N)} B = (2^{1/N} - 1)^{1/2} B_1. \quad (14)$$

These relationships are shown in Fig. 1 for  $N$  equals one, two, and eight, and infinity for the traveling-wave case.

There is also an interest in the variation of the gain with variation of the paramagnetic susceptibility. The logarithmic derivative of the total gain at resonance for  $N$  cascaded stages yields the following expression:<sup>3</sup>

$$\frac{dG}{G} = (G^{1/(2N)} - G^{-1/(2N)}) \frac{d\chi_0}{\chi_0}. \quad (15)$$

These relationships are given in Fig. 2, again for a traveling-wave amplifier ( $N = \infty$ ) and for a system of cascaded single-resonance circuits.

It is apparent from these relationships that only a few cascaded cavities can duplicate the behavior in gain-bandwidth and gain-sensitivity characteristics that a truly distributed traveling-wave amplifier would possess. The chief difference between the two configurations is tunability. A traveling-wave amplifier, as we have indicated above, is restricted in bandwidth only by the paramagnetic resonance line-shape, the RF bandwidth of the system presumably being many times this width. The bandwidth of the cavity structure is restricted not only by the paramagnetic line-shape but also by the tuning characteristic of the cavity. In the former case, one can tune electronically by changing the resonance frequency of the paramagnetic material through a change of magnetic field; in the latter case, a mechanical cavity tuning has to be made along with the magnetic tuning of the paramagnetic resonance.<sup>4</sup>

Both cavity and traveling-wave structures can be made unidirectional by the use of circular polarization.

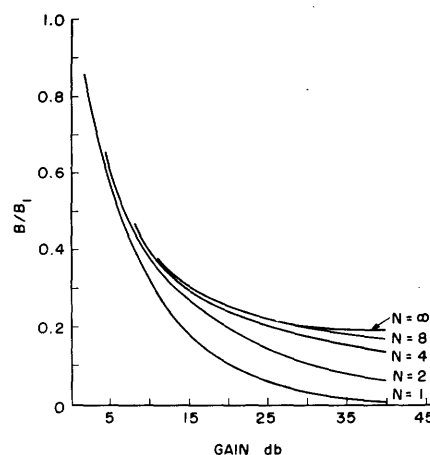


Fig. 1—Gain versus bandwidth curves as a function of the number of cascaded elements.

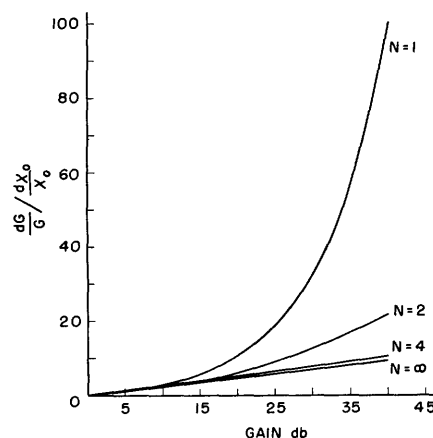


Fig. 2—Sensitivity of gain to variation of susceptibility as a function of the gain for varying numbers of cascaded elements.

This question has been discussed, and realizations for circuits have been given.<sup>5</sup> Here, we are mainly interested in suggesting an actual structure that is adaptable to a wide-frequency region; presumably, one that can utilize coaxial lines as transmission lines for the system.

The basic element of a circular-polarization system, as pointed out before,<sup>5</sup> is a cavity structure that has a degeneracy of modes arising from geometrical symmetry. The circular  $TE_{11n}$  mode has a degeneracy of two modes on axes  $90^\circ$  spatially separated, and hence this mode can be used to produce a circularly-polarized field. The field distributions of these cylindrical cavity fields are shown in Fig. 3(a). The corresponding fields in the square waveguide would be the  $TE_{01n}$  modes, which are shown in Fig. 3(b). If these two frequency-degenerate, spatially-orthogonal modes are driven  $\pi/2$  radians out of phase with each other in time, a pure circularly-polarized magnetic field will be produced along the axis of the cavity. This field becomes more and more elliptical as the cylindrical walls of the cavity are approached.

<sup>3</sup> R. L. Kyhl provided this form of (15).

<sup>4</sup> R. W. DeGrasse, E. O. Schulz-DuBois, and H. E. D. Scovil, "The three-level solid state traveling-wave maser," *Bell Sys. Tech. J.*, vol. 38, pp. 305-334; March, 1959.

<sup>5</sup> See, for example, M. Tinkham and M. W. P. Strandberg, "The excitation of circular polarization in microwave cavities," *Proc. IRE*, vol. 43, pp. 734-738; June, 1955.

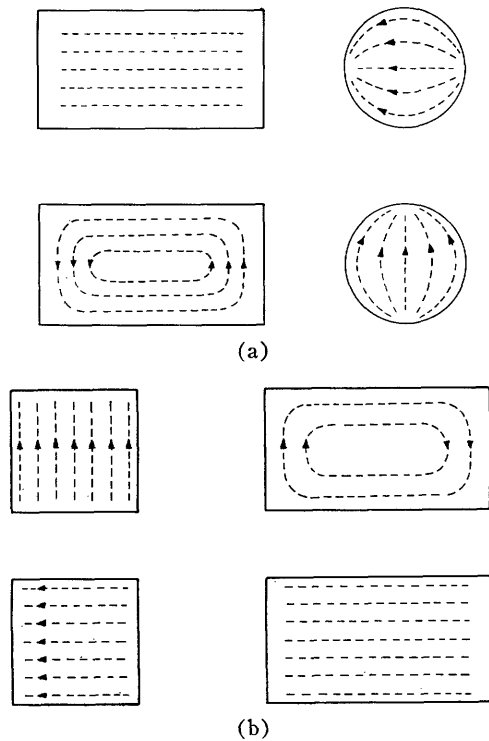


Fig. 3—(a) Radio-frequency magnetic-field configurations for the degenerate  $TE_{111}$  modes. (b) Radio-frequency magnetic-field configurations for the degenerate  $TE_{111}$  and  $TE_{101}$  modes.

However, even for a cavity uniformly filled with a paramagnetic crystal, one finds that the average square of the right and left circularly-polarized and longitudinal fields divided by the average square of the total field are:

$$\begin{aligned} \eta_+ \max &= 0.92(1 - \eta_z) \\ \eta_- \max &= 0.079(1 - \eta_z) \\ \eta_z \max &= \left[ 1 + 0.727 \left( \frac{Dn}{l} \right)^2 \right]^{-1} \end{aligned} \quad (16)$$

with

$$\eta_{\pm, z} = \frac{\int_{\text{crystal}} H_{\pm, z}^2 dv}{\int_{\text{cavity}} H^2 dv} \quad (17)$$

where  $D$  is the cavity diameter, and  $l$  is the length. The basic problem of exciting the circular-polarization field, then, is to achieve equality of field amplitude for these two orthogonal modes of the cavity through variation of the coupling coefficient to the transmission line feeding them and to have them time-phased  $\pm \pi/2$  radians.

Methods that use waveguides to achieve this coupling and phasing are rather abundant. A convenient method of obtaining such excitation with a cavity axis perpendicular to the feed waveguide has been given previously.<sup>5</sup> For frequencies lower than X-band frequencies, for example, it is convenient to use coaxial lines, especially for feedline structures which must be immersed in low-temperature dewars and inserted in magnetic fields. For this reason, we restrict our attention to excitation meth-

ods that can be achieved by using a coaxial line structure. It will be noted that each of these  $TE_{11n}$  modes can be fed by a separate coaxial line or waveguide, if a simple method of driving the two waveguides or coaxial line structures  $\pi/2$  radians out of phase can be realized.

This coupling of the two feed lines so that they are  $\pi/2$  radians out of phase with each other in time is readily accomplished by using a 3-db reactive or slot coupler. It is the property of a matched coupler that the two output fields which are established by the single input field must be  $90^\circ$  out of phase with each other in order to preserve the energy of the system. Therefore, if a 3-db, single-slot or multiple-slot matched coupler is used, the actual transmission line will be as shown in Fig. 4. The input coaxial line is coupled through a matched 3-db slot coupler into two feed transmission lines that are coupled directly into the two degenerate modes of the cavity. The energy reflected from the cavities, whether it is greater or less than the incident energy, will experience equal phase shift upon reflection from both cavity modes (we will indicate later how both modes can be made degenerate in their impedance characteristics so that this is so); hence, upon recombining in the 3-db coupler again the reflected energy goes entirely out the output line.

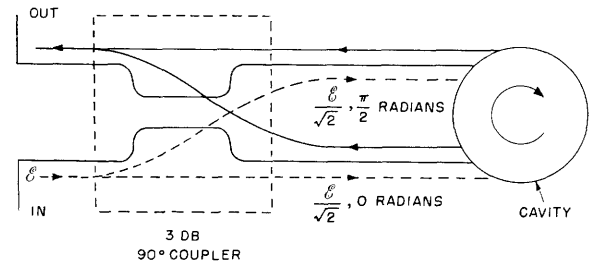


Fig. 4—Radio-frequency transmission line configuration for the 3-db coupler, circular-polarization excitor.

This structure is apparently reciprocal in the sense that energy coming in the output line is split in the 3-db coupler and sent down the two cavity transmission lines equally and with a  $\pi/2$  radian time-lag to set up the necessary circular-polarization field in the cavities. It will be noted, however, that in this case the polarization direction will be the negative of the one set up when the radiation impinges on the cavity from the input line. This is an important observation and is useful, as we shall see later on, in providing nonreciprocal gain. In any case, the fields reflected from the cavity, whether they are greater or less than the incident fields, will be recombined again in the 3-db slot coupler so as to emerge in toto from the input line.

The degree of unidirectionality depends, of course, upon how well the impedances of the two linear cavity modes are matched. With the two modes sharing a single absorbing or emitting crystal, the crystal losses or gains will be identical in both systems to the degree that the geometrical configuration of both modes is the same. In order for the impedance characteristics of the two modes

to be matched in frequency, they can be tuned to each other with small perturbing plugs which equalize the frequencies and  $Q$ 's of the two modes. Variation of the frequency and  $Q$ 's of the two degenerate modes with time will be identical because they are mutually inclusive structures. Thus, although a circular-polarization amplifier is in essence a bridge amplifier, since the amplifying cavities are mutually inclusive, the bothersome effects of drifts of gain characteristics are reduced to a minimum. An actual amplifier employing a ruby crystal is shown in Fig. 5.

#### TOLERANCE

As we indicated above, it is impossible to have a perfect circular-polarization amplifier unless the active material is restricted to an infinitesimal volume on the axis of the cavity itself. In a filled cavity, however, the ratio of the average of the two circular polarizations is large enough so that one circular polarization is in sufficient predominance for most practical cases. The actual interaction between the electromagnetic field and the crystal is measured by the product of quantum-mechanical operators  $|S_+|^2$ ,  $|S_-|^2$ , and  $|S_z|^2$  for the spin transition that is involved and, respectively, the electromagnetic field operators,  $H^2$ ,  $H_+^2$  and  $H_-^2$ . The ratio of the magnetic  $Q$  for the signal circular-polarization direction, (+), to the magnetic  $Q$  for the circular polarization of the opposite direction, (-), is thus given by the fraction

$$\frac{(Q_{x0})_-}{(Q_{x0})_+} = \frac{(\langle H_-^2 \rangle |S_+|^2 + \langle H_+^2 \rangle |S_-|^2 + \langle H_z^2 \rangle |S_z|^2)}{(\langle H_+^2 \rangle |S_+|^2 + \langle H_-^2 \rangle |S_-|^2 + \langle H_z^2 \rangle |S_z|^2)} \quad (18)$$

where the symbol  $\langle \rangle$  means an average over the crystal. Thus, using (16), with the cavity filled with a material exhibiting a perfect Faraday effect (*i.e.*, a material for which  $S_-^2 = S_z^2 = 0$ ) we can obtain a nonreciprocity of active or passive magnetic  $Q$  of 10.6 db. The resonant gain, (10) with  $\Delta f = 0$ , for either polarization is written directly as

$$\sqrt{G_{\pm}} = \frac{\frac{1}{Q_e} - \frac{1}{Q_0} - \frac{1}{Q_{x0\pm}}}{\frac{1}{Q_e} + \frac{1}{Q_0} + \frac{1}{Q_{x0\pm}}} \quad (19)$$

The gain equation can be manipulated into the form

$$\sqrt{G_{\pm}} = \frac{1 + \frac{Q_e}{Q_0} \left( \frac{Q_{x0-}}{Q_{x0+}} - 1 \right) - \frac{Q_{x0-}}{Q_{x0+}} \left( \frac{1 - \sqrt{G_+}}{1 + \sqrt{G_+}} \right)}{1 - \frac{Q_e}{Q_0} \left( \frac{Q_{x0-}}{Q_{x0+}} - 1 \right) + \frac{Q_{x0-}}{Q_{x0+}} \left( \frac{1 - \sqrt{G_+}}{1 + \sqrt{G_+}} \right)} \quad (20)$$

For a backward gain of the 1, the ratio of the magnetic  $Q$ 's in the forward and backward direction must be:

$$\frac{Q_{x0-}}{Q_{x0+}} = \frac{(0.78)^2 0.76 + (-0.069)^2 0.066 + (-0.65)^2 0.172}{(0.78)^2 (0.066) + (-0.069)^2 0.76 + (-0.65)^2 0.172} = 4.4 \quad (22)$$

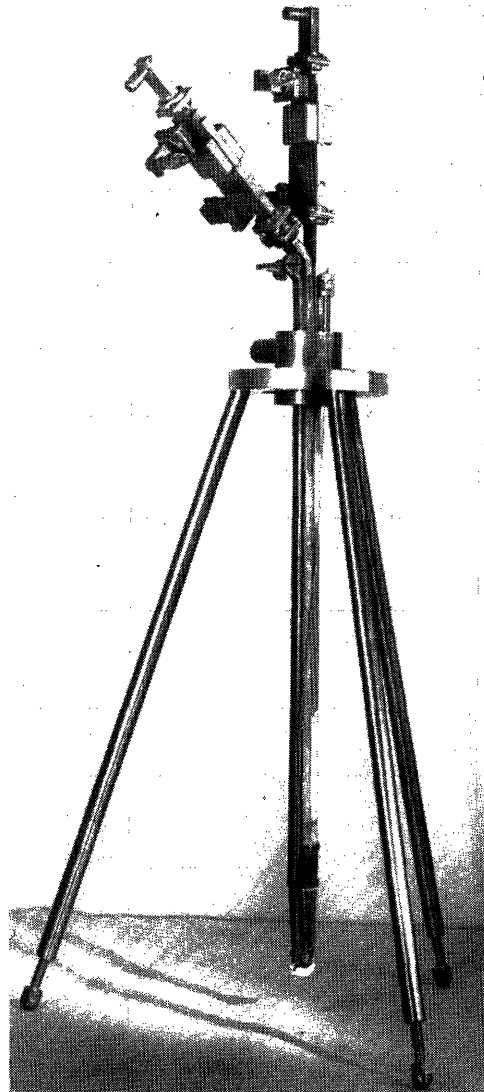


Fig. 5—An X-band circularly-polarized amplifier.

$$\frac{Q_{x0-}}{Q_{x0+}} = \frac{Q_0}{Q_e} \left( \frac{\sqrt{G_+} - 1}{\sqrt{G_+} + 1} \right) + 1. \quad (21)$$

This ratio of magnetic  $Q$ 's for the variation of  $\sqrt{G_+}$  from 1 to  $\infty$  is from 1 to  $1 + Q_0/Q_e$ , the latter limit being a separately controllable factor through the ratio  $Q_0/Q_e$ .

Actually, then, we need not require that the active material exhibit a perfect Faraday effect because a ratio of the two magnetic  $Q$ 's of 3 or 4 is sufficient to obtain, by (21), a gain nonreciprocity of  $\sqrt{G_+}$ . In fact, an X-band ruby amplifier designed with the magnetic field making an angle of  $70^\circ$  with the crystalline  $c$  axis and with the circular polarization vector itself and at a field of approximately 3.8 kilogauss operating between the two highest energy levels, as indicated in Fig. 6, will have a ratio  $S_+ : S_- : S_z = 0.78 : -0.069 : -0.65$ . Thus, the ratio  $(Q_{x0})_- / (Q_{x0})_+$  in a  $TE_{111}$  cavity is for  $D/l = 2.58$ ,

and hence the reverse gain is one, or less, for a  $Q_0/Q_c$  ratio of 3.5, or less. At first sight it might seem that this arrangement would have very poor directional properties because the magnetic field makes such a large angle with the actual circular-polarization axis. That this is not the case is merely an indication that the quantum-mechanical mixing and transition probabilities are not intuitively evident.

The effect of reflection in the output line on the stability of the amplifier using this circular-polarization structure can be considered. It is evident that nonreciprocity is of tremendous assistance in reducing the effect of the reflections on the amplifier gain. If we call the reflection coefficient in the output and input arms  $r_o$  and  $r_i$ , the actual gain of the device is

$$\frac{G_+}{(1 - \sqrt{G_+ G_-} r_o r_i)^2} \quad (23)$$

A typical value of  $\sqrt{G_+}$  is 10 (20-db gain) and of  $\sqrt{G_-}$  is 1. This means that for a gain stability of  $\pm 10$  per cent for all phases of the reflection coefficients the magnitude of reflection coefficients in both the input arm and the output arm will be required to be less than 0.07. A reciprocal amplifier would, of course, require that the reflection coefficients in this case be less than 0.02. This improvement is more spectacular when stated in terms of VSWR: the nonreciprocal amplifier requires a VSWR of less than 1.14 in input and output arms, but the reciprocal amplifier (using an external isolator circulator) requires a VSWR of 1.04 or less with the same forward gain condition.

The further advantage of nonreciprocity in a unidirectional amplifier stems from its insensitivity to noise radiated from the output load. This noise is characterized by the temperature of the output load, which would be about 300°K. This temperature,  $T_L$ , is not to be confused with the effective noise temperature of the second stage,  $T_0$ , since this temperature,  $T_0$ , includes the effect of conversion losses in this stage. The noise from the output terminal characterized by  $T_L$  is amplified by the paramagnetic system to give  $G_- T_L$  at the input. Reflections in the input arm,  $r_i$ , then increase the apparent source noise temperature by  $r_i^2 G_- T_L$ . For this to be only a few degrees Kelvin, with  $G_- \approx 1$ ,  $r_i \leq 0.1$ . This means that the antenna or input VSWR must be less than 1.2, which is readily achieved. With a unidirectional reciprocal amplifier operating with a circulator, the same analysis yields  $r_i \leq 0.1\sqrt{c/G_-}$ , or  $\text{VSWR} \leq 1 + (0.2\sqrt{c/G_-})$ , where  $c$  is the reverse loss of the circulator.

#### DESIGN FEATURES

The design of a circular-polarization cavity requires that attention shall be paid to the cylindrical symmetry of the system. For example, since some paramagnetic crystals, such as ruby, are anisotropic in electric susceptibility, one must try to have a crystal with its  $c$ -axis as parallel to the cavity axis as possible. Even this is

not a great restriction; with ruby, the difference in the index of refraction means essentially that if the crystal axis is 5° off the cylinder axis the two modes in the cavity will not be degenerate by approximately 100 mc. This can be of the order of magnitude of perturbations of other asymmetries in the system, so that one can readily align the crystal to the cavity axis sufficiently accurately. Small tuning plugs that change both frequency and cavity  $Q$ 's (by introducing resistive loss into the one cavity selectively) can then be used to obtain balance of the two mode impedances.

An additional problem encountered in saturation paramagnetic amplifiers, is the introduction of the pumping power. This saturating power is introduced in our amplifier through a  $K$ -band waveguide, slot-coupled to the cavity midway between the two amplifier coupling irises. The slot is a large one, essentially resonant at the pumping frequency. At a symmetrical point,  $\pi/2$  radians in space, a dummy coupling iris is introduced in order to compensate for the mode-splitting effect of the pumping iris.

In discussions of this type of amplifier, it seems not to be realized that the amplifier cavity need not be made resonant at any particular pump frequency, since tuning elements of the pump feed guide can be used to resonant the over-all structure, which comprises guide, coupling window, and amplifier cavity, to the pumping electromagnetic radiation. In the present amplifier, we do not need to be as sophisticated as this; there are many available  $K$ -band resonances. A glance at a cavity mode chart is convincing on this point. With an anisotropic dielectric constant, the usual cylindrical cavity mode chart is not directly applicable, but, between  $K$  and  $K_A$  bands, several dozen resonances are available. In this case, one need only arrange the static field and its angle with the crystal-axis to be proper for the amplifier and pump frequency cavity resonances to coincide with the spin system resonances. For example, using ruby, as shown in Fig. 6, for variation of the static field from 2 to 3.8 kg and the simultaneous variation of angle between the field and  $c$  axis from 55° to 70°, we find the amplifier resonances to be constant at 9 kmc, while the necessary pump varies from 23 kmc to 36 kmc. The ratio of forward to backward negative  $Q$  does not vary greatly with these changes in operating conditions.

There is also no need to restrict the active crystal to regions of high-pumping electromagnetic field. As has been pointed out in the literature, an inhomogeneous electromagnetic field can give rise to homogeneous polarization of the amplifier levels since several mechanisms exist to give energy transport within the crystal.<sup>6</sup> If this were not so, only a small filling factor could be obtained, because the paramagnetic crystal would have to be limited to those points in the amplifier at which

<sup>6</sup> R. J. Morris, R. L. Kyhl, and M. W. P. Strandberg, "A tunable maser amplifier with large bandwidth," *Proc. IRE*, vol. 47, p. 80; January, 1959.



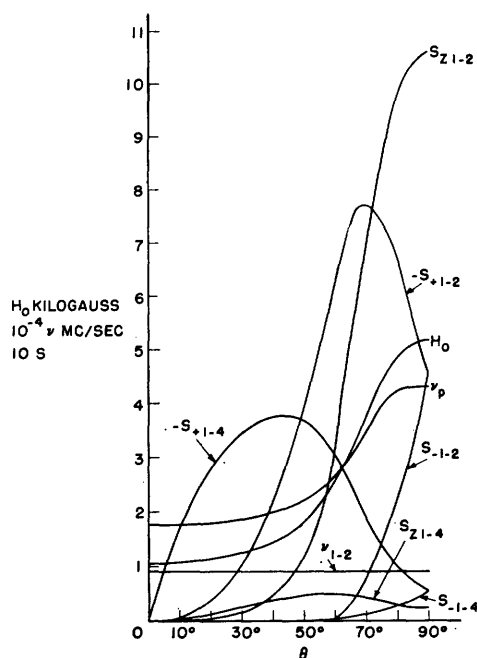


Fig. 6—Operating parameters curves for amplification on the two highest energy ruby levels, with pumping from the top to the bottom level.

the pumping field had a large amplitude. Thus, the possibility of phonon (or other) transport of pumping energy within the amplifying crystal tremendously simplifies the design of the pumping cavity mode. Any means of tuning the coupling waveguide, coupling iris, and cavity to match the pumping power into the crystal may be used, since the important factor is the actual power transfer to the crystal and not the mode configuration. This is not a reckless gesture with the pumping power, as so little power (hundreds of microwatts), matched into the crystal, is needed in a properly designed amplifier. Furthermore, the absence of a restriction on placing the active crystal on the vicinity of pumping-field nodes means that the whole cavity can be filled with a crystal. This gives a maximum filling-factor  $\eta$  and lowest magnetic  $Q$  and hence greatest gain-bandwidth product for the amplifier.

#### QUANTUM-MECHANICAL DESIGN

In order to test the feasibility of these suggestions, two amplifiers were constructed embodying the principles involved. One operates at  $X$  band (3 cm), using a waveguide structure, and the other at  $L$  band, using coaxial lines. The  $L$ -band amplifier presents somewhat different problems from those of the  $X$ -band amplifier, most of which are simply problems of translating waveguide structures into coaxial line structures and have been solved at this point. The 3-db coupler, which was designed by using stripline techniques, presents no difficulty. Instead of using a circular  $TE_{111}$  cavity at  $L$  band as a mutually inclusive structure, it was decided to use two geometrically-orthogonal quarter-wave stripline cavities, as indicated in Fig. 7. These two ortho-

nal resonance structures share a common crystal. The filling factor achievable by this technique is about one-third, but this is sufficient to yield an amplifier for operation at the hydrogen line frequency which should have a bandwidth of 100 kc with a gain of 30 db. The possibility of operating such a device without a circulator is indeed exciting, especially for radioastronomy purposes. Circulators that are available in this frequency region have insertion losses of approximately 0.2 db.

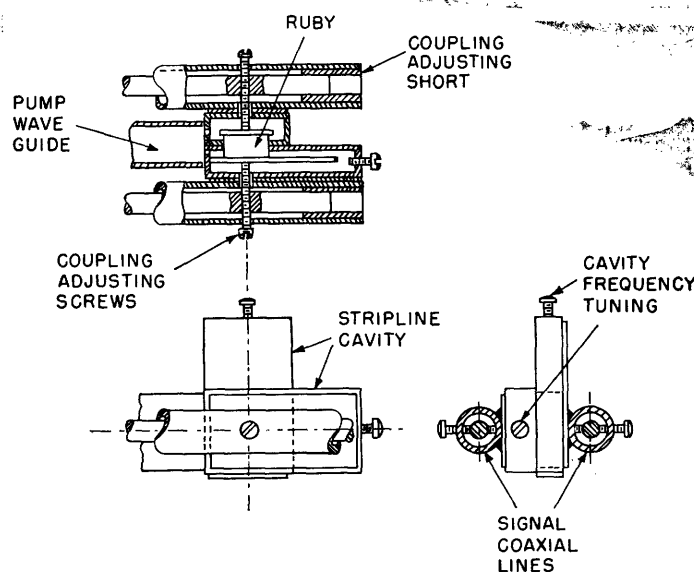


Fig. 7—Stripline, orthogonal-cavity, circularly-polarized amplifier for  $L$ -band.

This gives a limiting amplifier temperature of 14°K, an order of magnitude greater than the intrinsic temperature of the amplifier. Hence, one would expect an order of magnitude improvement in the sensitivity of a radio telescope equipped with such an intrinsically unidirectional amplifier over that obtainable with the reciprocal amplifier-lossy circulator combination. Since tests of this amplifier are not finished, the following description will be restricted to a discussion of the design and operation of the  $X$ -band amplifier.

It was decided at the start, to make the test amplifier in a structure with an intrinsic  $Q$  limited by dielectric  $Q$  of ruby at low temperature. It is our experience that this limiting ruby  $Q$  at helium temperatures and  $X$  band is around 3000. It will be seen later that such a  $Q$  is an order of magnitude greater than the achievable magnetic  $Q$  of ruby operated at this temperature. However, we felt that if a high- $Q$  structure could be made to behave properly as a circularly-polarized amplifier, then it would be less work to eliminate the difficulties encountered with lower- $Q$  systems. As it turned out, no difficulty was encountered in operating the device, even with a  $Q$  of several thousand, if a few relatively simple precautions were taken. The ruby  $c$  axis was aligned to within one degree of the cylinder axis by the method of



Unfortunately, our present understanding of the spin-lattice transition matrix elements, the  $w$ 's in the equations above, is based for the most part on theoretical considerations. The experiments that have been performed on paramagnetic systems such as ruby have measured a spin-lattice relaxation time that is essentially a measure of the net interaction due to all of these transition probabilities. It is sufficient to say that the major interaction of the lattice with the spin comes through the crystalline electric field.<sup>11</sup> The dominant spin-dependent term, in this case, yields  $w$ 's that depend upon the square of the spin anticommutator:

$$w_{ij} \propto |S_\alpha S_\beta + S_\beta S_\alpha|_{ij}^2 \quad \alpha, \beta = x, y, z. \quad (27)$$

For example, between the pure spin states of  $S_z = \pm \frac{1}{2}$ , this operator vanishes, and as a consequence these spin levels should have a small  $w_{ji}$ , or a long spin-lattice relaxation time. That the selection of operating point on the basis of most favorable spin-lattice relaxation ratios is an important consideration may be seen as follows. If our present understanding of the spin-lattice relaxation process is correct, one may introduce the following relationships which must exist in paramagnetic systems having nearly pure spin spatial quantization (e.g., in ruby with a magnetic field parallel or nearly parallel with the  $c$  axis):

$$\begin{aligned} w_{41} &\approx 0 \approx w_{32} \\ w_{43} &\approx w_{21}. \end{aligned} \quad (28)$$

The minimum ratio of pump to amplifier frequency is then given by (25) as

$$\frac{f_{\text{pump}}}{f_{\text{amp}}} = \frac{2w_{21}w_{42} + w_{21}^2}{w_{21}w_{42} + w_{21}^2}. \quad (29)$$

We have not, as yet, computed the local normal lattice modes for chromium in ruby, but it is reasonable to think that the allowed transitions will have comparable magnitudes. With the spin-lattice relaxation time for the 42 levels approximately equal to that of the 21 levels, we are led to believe that a pump-to-amplifier frequency ratio of only 3/2 is necessary for operation near the region where the spin-projection quantum numbers  $S_z$  are reasonably good. They cannot be perfect quantum numbers, obviously, because this would mean that the pumping transition would not be allowed. On the other hand, the rate of growth of the spin-lattice relaxation probability,  $w_{-1/2, +1/2}$ , between the  $+\frac{1}{2}$ ,  $-\frac{1}{2}$  levels is identical with that of the coupling between the pumping field and the spin levels. This means that a convenient compromise between a small  $w_{-1/2, +1/2}$  and a small pumping  $Q_{x0}$  can be arranged. For example, in ruby with the magnetic field of eight kilogauss at approximately  $5^\circ$  from the crystal axis, one should be able to operate an amplifier at  $\nu_{23} = 22$  kmc with a pump at  $\nu_{24} = 34$  kmc.

<sup>11</sup> R. D. Mattuck, "Phonon-Spin Absorption in Paramagnetic Crystals," Ph.D. Thesis, Department of Physics, M.I.T.; June 1959; also, R. D. Mattuck and M. W. P. Strandberg, "Quadrupole Selection Rule," *Phys. Rev. Letter* 3, p. 369; October 15, 1959; also R. D. Mattuck and M. W. P. Strandberg, "Spin-phonon interaction in paramagnetic crystals," *Phys. Rev.* (to be published).

For all of the reasons outlined above, the actual ruby amplifier operating point should be determined from Fig. 8, keeping in mind the desirability of a high pump-to-amplifier-frequency ratio, large amplifier matrix elements, the greatest difference between the  $S_+$  and  $S_-$  matrix elements for the amplifier transition, and the use of those amplifier levels most nearly characterized by the  $S_z$  quantum numbers of  $\pm \frac{1}{2}$ . The most appropriate operating point would be around  $\theta = 20^\circ$  with a pump at about 31 kmc. The actual tests of the amplifier structure were made at  $\theta = 45^\circ$  and  $\theta = 55^\circ$ , since available pump oscillators were limited to the frequency region between 22 and 26 kmc.

## RESULTS

The circular polarization structure showed little fundamental difficulty in obtaining proper performance. There was some splitting of the modes on cooling (a few megacycles) but this was corrected by a rocking tuner arm that could be used to tune either one or the other mode to a lower frequency. As shown in Fig. 9, the device was arranged with circulators in order to separate the incident and reflected signals. In operation at the  $55^\circ$  orientation the ratio of the magnetic  $Q$ 's for the two directions of circular polarization is shown in Fig. 10. With the amplifier signal on the  $A$  terminal, the transmitted power detected at the  $a$  crystal is shown on the top trace of the oscilloscope picture; with the signal on the  $B$  terminal, the transmitted power is shown on the bottom trace. Of course, with the signal on the  $A$

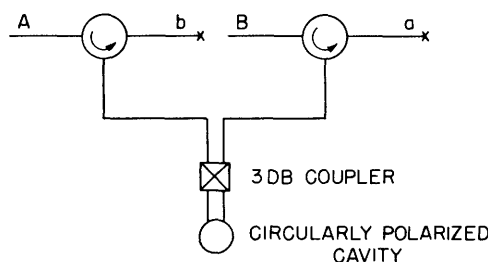


Fig. 9—Circularly-polarized amplifier test signal paths.

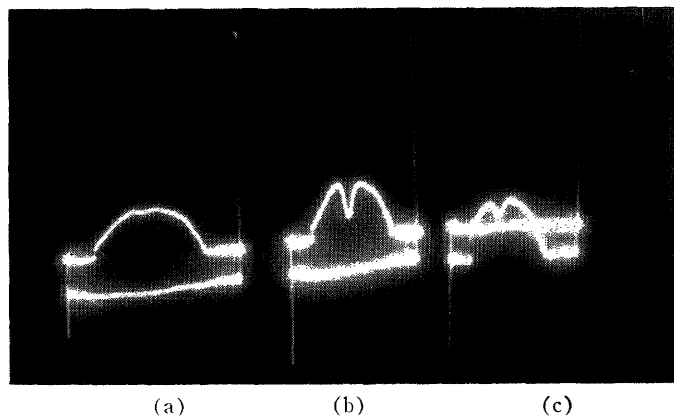


Fig. 10—Signal klystron mode curves. (b) the pumping klystron turned off and the paramagnetic transition resonance off cavity resonance; (a) the paramagnetic resonance on resonance and the signal on terminal  $A$ ; (c) the signal on  $B$ . In each picture the upper trace of the double-trace presentation is from crystal  $a$  and the lower trace is from crystal  $b$ .

terminal, the  $b$  crystal (the lower trace) detects the reflected power. The ratio of the forward and backward magnetic  $Q$ 's is obviously large. In the forward direction, the magnetic  $Q$  is much smaller than the off-resonant loaded  $Q$  of the cavity (3000); the reverse magnetic  $Q$  is of the order of 4000. Operation with the pump power on, led only to oscillation since the external  $Q$  was much larger than the magnetic  $Q$  of the crystal. In order to obtain amplifier action, it was necessary to operate the amplifier with a high signal input. This has the effect of increasing the magnitude of the magnetic  $Q$  by reducing a difference in populations of the amplifier levels. The effect of the large signal power is essentially to increase  $w_{23}$  in the denominator of (25) or (26) in proportion to the signal power. The operating characteristics of the amplifier can be seen from Fig. 11. With the signal introduced through the forward direction, the forward gain was large; with the signal introduced in the reverse direction, the reflection gain was large, while the forward gain was actually a loss. The directionality indicated is apparently even greater than the amplifier gain itself.

The magnetic  $Q$  can only be estimated from the signal saturation power, which was in the  $10\text{ }\mu\text{w}$  region, and would indicate a negative magnetic  $Q$  of approximately 300. Since this is the order of the absorption  $Q$  at  $4^\circ\text{K}$ , the amplifier temperature must likewise be of the order of  $4^\circ\text{K}$ .

#### CONCLUSION

The physical parameters which enter into the design of paramagnetic quantum-mechanical amplifiers have been discussed. It has been shown that the most crucial

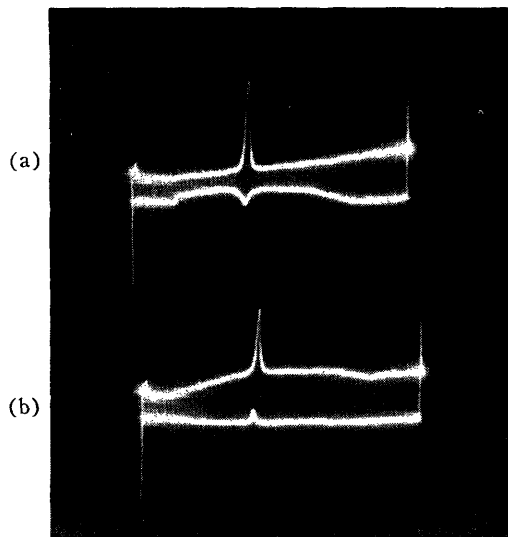


Fig. 11—Circularly-polarized amplifier in operation with pump radio-frequency turned on, and  $\theta = 55^\circ$ . The signal level is high so that the amplifier is operated at its saturation point in order to increase the magnitude of the paramagnetic  $Q$  to a value at which the amplifier does not oscillate. The two lower traces show the detected current at crystal  $a$  on (a), and crystal  $b$  on (b) for the signal on the  $A$  terminal. The two upper traces show the same crystal signals with the signal on the  $B$  terminal. The reflection that is being amplified arises from the thin teflon window at the amplifier output.

elements in the amplifier design are reducible to analytical expressions. It has been especially demonstrated that regenerative cavity amplifiers can be made unidirectional, with obvious simplicity, and that a simple cascade of such amplifiers can give operational characteristics similar to those of traveling-wave devices. It has been indicated that unidirectional regenerative amplifiers can have noise figures an order of magnitude less than the noise figures of cavity amplifiers requiring circulators for isolation of input and output because the noise temperature for the amplifier increases with circulator loss at a rate of  $7.2^\circ\text{K}$  per 0.1-db loss in the circulator. The relaxed specification for input and output reflection coefficient should also yield more stable amplifier gain characteristics; even with a circulator, the reflection coefficients of the circulator must be reduced to a very low level when a reciprocal amplifier is being used, or the electrical-line length between amplifier and circulator must be very well stabilized. This is quite difficult to accomplish, especially in transmission lines filled with an amount of liquid helium, which varies with time.

The selection of the type of amplifier—a single-cavity regenerative amplifier, a cascade of cavity amplifiers, or a slow-wave structure—is to be determined by the end use of the amplifier. No single amplifier type is fitting for all applications. For uses requiring wide tunability and moderate gain-bandwidth product, the regenerative-cavity configuration is probably most effective. For wide-band high-gain purposes, cascaded cavities or a slow-wave structure will have to be used. The latter device requires more engineering development and is less conveniently tuned over a wide frequency region. It is most important to note that a single regenerative cavity can never have a gain-bandwidth product greater than twice the intrinsic paramagnetic linewidth. From this point of view, it seems futile to try to achieve magnetic  $Q$ 's which are much smaller than the operating frequency divided by the paramagnetic linewidth. The linewidth can be increased if we increase the concentration of the paramagnetic ions with a rapid increase of other deleterious effects, such as the cross relaxation between the paramagnetic energy levels. This effect decreases the spin-lattice relaxation time and rapidly increases the required pumping power. Alternatively, the linewidth may be broadened by making the magnetic field inhomogeneous or by using more than one crystal in the structure, each crystal having a separate alignment with respect to the magnetic field. Unless these measures are consciously carried out, it would seem incredible that gain-bandwidth products in excess of 100 mc could be achieved at any foreseeable microwave frequency.

#### ANALYTICAL APPENDIX

The energy levels of a paramagnet are determined from a spin-Hamiltonian  $\mathcal{H}$ , which essentially expresses the three-dimensional rotational transformation properties of the spin system as defined by the symmetry of its

crystalline environment. It may be expressed as a power-series expansion in the operators of the static field,  $\mathbf{H}_0$ , and the spin,  $\mathbf{S}_x$ ,  $\mathbf{S}_y$ , and  $\mathbf{S}_z$ . The expansion is truncated at the spin term expressing the lowest symmetry of the system and with the field and spin terms first power in the field. The latter truncation is for simplicity and is a reasonable approximation in general. For ruby, with the  $\text{Cr}^{+++}$  ion in a crystal site having trigonal symmetry, the form this expansion takes is

$$(\mathcal{H}) = g_{\parallel}\beta_0 H_0 \cos \theta (\mathbf{S}_z) + g_{\perp}\beta_0 H_0 \sin \theta (\mathbf{S}_{x,y}) + D[(\mathbf{S}_z^2) - \frac{1}{3}S(S+1)(\mathbf{I})] \quad (30)$$

where

$g_{\parallel}$  = magneto-gyric conversion factor parallel to  $c$  axis

$g_{\perp}$  = magneto-gyric conversion factor perpendicular to  $c$  axis

$\beta_0$  = the Bohr magneton =  $1.4 \cdot h$  mc/gauss, where  $h$  is Planck's constant

$H_0$  = applied static-magnetic field magnitude in gauss

$\theta$  = angle between  $\mathbf{H}_0$  and  $c$  axis

$2D$  = zero field crystalline splitting =  $-11,470$  mc

$S = 3/2$ , the maximum spin-projection quantum number

$(\mathbf{S}_{x,y})$  = either the  $\mathbf{S}_x$  or  $\mathbf{S}_y$  matrix

$$\mathbf{S}_z = \begin{bmatrix} \frac{3}{2} & 0 & 0 & 0 \\ 0 & \frac{1}{2} & 0 & 0 \\ 0 & 0 & -\frac{1}{2} & 0 \\ 0 & 0 & 0 & -\frac{3}{2} \end{bmatrix}$$

$$\mathbf{S}_x = \begin{bmatrix} 0 & \sqrt{\frac{3}{2}} & 0 & 0 \\ \sqrt{\frac{3}{2}} & 0 & 1 & 0 \\ 0 & 1 & 0 & \sqrt{\frac{3}{2}} \\ 0 & 0 & \sqrt{\frac{3}{2}} & 0 \end{bmatrix}$$

$$\mathbf{S}_y = \begin{bmatrix} 0 & i\sqrt{\frac{3}{2}} & 0 & 0 \\ -i\sqrt{\frac{3}{2}} & 0 & i & 0 \\ 0 & -i & 0 & i\sqrt{\frac{3}{2}} \\ 0 & 0 & -i\sqrt{\frac{3}{2}} & 0 \end{bmatrix}$$

$$\mathbf{I} = \begin{bmatrix} 1 & 0 & 0 & 0 \\ 0 & 1 & 0 & 0 \\ 0 & 0 & 1 & 0 \\ 0 & 0 & 0 & 1 \end{bmatrix}$$

The characteristic energies of this matrix are those of its diagonal representation, or, explicitly, the energies that make the secular determinant formed from the Hamiltonian equal to zero. Symbolically,

$$|\mathcal{H}_{ij} - \delta_{ij}\lambda_{ij}| = 0, \quad \text{with } \delta_{ij} = \begin{cases} 1, & i = j \\ 0, & i \neq j \end{cases} \quad (31)$$

The process for solving the secular determinant may be considered the same as the process used in finding an orthogonalized transformation  $\mathbf{T}$  such as the  $\mathbf{T}\mathcal{H}\mathbf{T}^{-1} = \boldsymbol{\lambda}$ , where  $\boldsymbol{\lambda}$  is the diagonal matrix  $|\delta_{ij}\lambda_{ij}|$ . The methods for diagonalizing this form of matrix and for determining the transformation  $\mathbf{T}$  have been given.<sup>2</sup> For convenience, the spin Hamiltonian is tabulated in terms of a natural, or crystalline, coordinate system, the static magnetic field  $\mathbf{H}_0$  having any orientation with respect to these axes. In general, then, the transformation  $\mathbf{T}$  will vary not only with the magnitude of  $\mathbf{H}_0$  but also with its orientation with respect to the spin-Hamiltonian axes.

The interaction energy of a spin of a paramagnetic ion with an RF magnetic field is also given to first order in terms of the spin-magnetic moment  $\mathbf{u}$  and the RF magnetic field  $\mathbf{H}$  having a frequency  $f$ , as:

$$\mathcal{H}_{\text{interaction}} = -\mathbf{u} \cdot \mathbf{H} \cos 2\pi f t \quad (32)$$

with

$$-\mathbf{u}_{x,y,z} = g_{x,y,z}\beta_0 \mathbf{S}_{x,y,z} \quad (33)$$

One may show that, in general, a system having a phase-memory time  $\tau$  (spin-spin relaxation time)  $= (\pi B_x)^{-1}$  has a magnetization when perturbed by  $\text{Re}(-\mathbf{u} \cdot \mathbf{H} e^{-i2\pi f t})$  of<sup>2</sup>

$$\mathbf{M}(t) = \sum_{ij} \mathbf{u}_{ji} (\mathbf{u}_{ji} \cdot \mathbf{H} e^{-i2\pi f t}) \left( 1 - \frac{f}{f - f_{ij} + i\frac{B_x}{2}} \right) \frac{N_i - N_j}{2hf_{ij}} + \sum_{ij} \mathbf{u}_{ji} (\mathbf{u}_{ij} \cdot \mathbf{H} e^{i2\pi f t}) \left( 1 - \frac{f}{f - f_{ij} - i\frac{B_x}{2}} \right) \frac{N_i - N_j}{2hf_{ij}} \quad (34)$$

where  $h$  is Planck's constant,  $B_x$  is the line frequency width, and  $N_i$  and  $N_j$  are the number of spins per  $\text{cm}^3$  in levels  $i$  and  $j$ . We may neglect the second term on the right as a non-resonant high-frequency contribution to the susceptibility. Using Cartesian components of  $\mathbf{u}$ , it will be seen that  $M_x$  depends upon both  $H_x$  and  $H_y$ , yielding a non-diagonal tensor susceptibility.

The  $-\mathbf{u}_{\pm} = \beta_0(g_x \mathbf{S}_x \pm ig_y \mathbf{S}_y)/\sqrt{2}$ ,  $\mathbf{H}_{\pm} = (\mathbf{H}_x \pm i\mathbf{H}_y)/\sqrt{2}$  operators are convenient in that they simply exhibit the

circular-polarization properties of the system, and incidentally yield a diagonal tensor susceptibility under some conditions. In general, the susceptibility tensor is not diagonal. However, since we are interested in the circuit averages of  $\mathbf{H} \cdot d\mathbf{M}^*$ , the off-diagonal terms average to zero by symmetry or design in cavity systems. Thus, one need use only the diagonal terms expressed as (since  $(S_{\pm})_{ij}(S_{\mp})_{ji} = |S_{\pm}|_{ij}^2$ ):

$$\mathcal{Q}_z^{-1} = \frac{4\pi \left[ \chi_+ \int_{\text{crystal}} H_-^2 dv + \chi_- \int_{\text{crystal}} H_+^2 dv + \chi_z \int_{\text{crystal}} H_z^2 dv \right]}{\int_{\text{cavity}} H^2 dv} = 4\pi [\chi_+ \eta_+ + \chi_- \eta_- + \chi_z \eta_z] \quad (37)$$

$$\chi_{\pm,z} = \frac{M_{\pm,z}}{H_{\pm,z}^*} = g^2 \beta_0^2 \sum_{ij} |S_{\pm,z}|_{ij}^2 \cdot \left[ 1 - \frac{f}{f - f_{ij} + i \frac{B_x}{2}} \right] \frac{N_i - N_j}{hf_{ij}}. \quad (35)$$

The factor 1 gives rise to the static susceptibility, which we neglect since it is 500 times smaller than the resonant factor at X-band frequencies.

If we are interested in the susceptibility arising from two levels of a system, say  $i$  and  $j$ , as the magnetic field changes magnitude and orientation, we must study the transformation properties of the spin angular-momentum components upon which the magnetic moment depends:

$$(S'_{\pm,z})_{ij} = \mathbf{T} S_{\pm,z} \mathbf{T}^{-1}. \quad (36)$$

These elements have been given by Davis and Strandberg for the case  $S=3/2$  with trigonal symmetry.<sup>8</sup> We merely note that the transformation properties of this electromagnetic coupling term may be studied for the general case in terms of the three-dimensional finite rotational properties of the spin Hamiltonian,<sup>12</sup> or by the simple expedient (if rapid-computing facilities are available) of computing the interaction operator for various magnetic-field magnitudes and orientations. Though the zero-interaction field angle (*i.e.*, the orientation angle for the RF field for no interaction with the quantum mechanical system) exists at a discrete angle, care must be taken to understand these coupling matrices to avoid this angle. We have indicated a splendid mistake of this kind in which the RF field was mistakenly oriented along the zero interaction angle.<sup>13</sup> The fact that the device operated almost as expected (the required pumping power was, in fact, too much) was due only to

other fairly subtle and esoteric effects that are, as yet, not fully understood.

We may define a circuit, or effective, complex susceptibility,  $\chi = \chi' - i\chi''$ , and hence a complex magnetic  $\mathcal{Q}_z$  in terms of the crystal susceptibility averaged over the whole circuit with a weighting factor of the square of the RF magnetic-field components (since energy loss and storage are proportional to the field squared):

where  $\eta$  = filling factor: in the denominator, we may neglect the effect of  $\chi'$  on the stored energy because it is zero on resonance, the condition that we are investigating, and usually is negligible on off-resonance in paramagnetic materials.

For nonreciprocity, we want the factors contributing to  $\chi_+ \eta_+$  (or  $\chi_- \eta_-$ ) to be large as compared to the other factors so that, as direction of propagation is reversed and  $H_+ \rightarrow H_-$  (or  $H_- \rightarrow H_+$ ), the RF coupling term is reduced by a large factor. Note that  $H_+$ ,  $H_-$ , and  $H_z$  refer in our case to the natural crystal axes simply because we represented  $\mathcal{H}$  in terms of these axes. Since we must use TE modes to obtain circular polarization in the method presented here, an  $H_z$  component must always exist. Thus, the breakdown of a pure Faraday effect, *i.e.*,  $(-\mathbf{u} \cdot \mathbf{H}_{\text{RF}})$  not proportional to  $H_+$ , may not be due to a growth of interaction with the  $H_-$  component so much as to a growth of the interaction with the  $H_z$  component. Evidently, the polarization axis for the maximum ratio of the backward-to-forward interaction is not restricted to the crystalline-field axis for general static magnetic-field magnitude and orientation. The optimum axis is found by studying the effect of the three-dimensional finite rotation operators required to change the quantization axes to other than the crystalline magnetic axes.<sup>12</sup> We do not discuss this topic here because such an optimization of the nonreciprocity is experimentally difficult in an anisotropic crystal such as ruby. Establishing a circularly-polarized field off the crystal axis is very difficult in the presence of anisotropy. Since we can achieve our results without the extra effort of optimizing them, we have gratefully chosen expediency to elegance and polarized along the  $c$  axis.

For application of these results to amplifiers, we need to express the gain-bandwidth product, the pumping power, and the noise figures in terms of them. From (12) we have

$$\sqrt{GB} = \frac{2}{\frac{1}{B_x} + \frac{Q_{x0}}{f_0}}. \quad (38)$$

<sup>12</sup> M. W. P. Strandberg, "Cross-over Transitions," Ninth Quarterly Progress Report on Contract No. DA36-039-sc-74895, Research Laboratory of Electronics, M.I.T.; Aug. 15, 1959–Nov. 15, 1959.

<sup>13</sup> M. W. P. Strandberg, C. F. Davis, Jr., B. W. Faughnan, R. L. Kyhl, and G. J. Wolga, "Operation of a solid-state quantum-mechanical amplifier," *Phys. Rev.*, vol. 109, pp. 1988–1989; March 15, 1958.

The activation pumping power can be computed by noting that in steady state the power into the pumped levels of the crystal must be equal to the power which is transferred to the crystal lattice because of spin-lattice relaxation. The rate at which the spin returns to thermal equilibrium population is conventionally measured by a time  $\tau_1$ , the spin-lattice-relaxation time. Without entering into a critical discussion of the meaningfulness of the

But

$$|Q_{x0}|_{\text{amplification}} = f_0 \left[ \frac{2}{\sqrt{GB}} - \frac{1}{B_x} \right], \quad (44)$$

the right-hand side of the equation being conveniently measurable.

The minimum matched-output noise figure,  $F$ , is then determined from the following:

$$F = \frac{\text{(noise power available at the output)}}{G \text{(noise power available at antenna when matched to load at } 290^\circ\text{K)}} \\ F = \frac{1}{290^\circ} \left[ \frac{(\sqrt{G} + 1)^2}{G} \left\{ T_s + \frac{Q_e}{Q_0} [T_e + |T_x|] + \left( \frac{\sqrt{G} - 1}{\sqrt{G} + 1} \right) |T_x| \right\} + \frac{T_0}{G} \right] \quad (45)$$

parameter,<sup>14</sup> we note that the spin-lattice transition rate is defined as

$$\left[ \frac{d(N_i - N_j)}{dt} \right] \\ = - \frac{(N_i - N_j) - (N_i - N_j)_{\text{equilibrium}}}{2\tau_1}. \quad (39)$$

When levels  $i$  and  $j$  are saturated, *i. e.*, when  $N_i \approx N_j$ , the energy is transferred at a rate

$$hf_0 V \left[ \frac{d(N_i - N_j)}{dt} \right] = hf_0 \frac{V(N_i - N_j)_{\text{equilibrium}}}{2\tau_1} \quad (40)$$

where  $V$  is the crystal volume. In terms of  $Q$ 's and the total stored energy  $U$ , we have

$$P_{\text{in}} = \frac{2\pi f_0 U}{Q_0} + \frac{(N_i - N_j)_{\text{equilibrium}} hf_0 V}{2\tau_1} \\ = \frac{2\pi f_0 U}{Q_0} + \frac{2\pi f_0 U}{Q_{x0}}. \quad (41)$$

In order to match most of the power into the spins rather than into the cavity walls,  $Q_{x0 \text{ pump}}$  must be much less than  $Q_0$  so that saturation will be reached when  $Q_{x0} \approx Q_0$ , *i. e.*, when half the pump power is absorbed by the cavity walls. Thus,

$$P_{\text{in}} \approx \frac{(N_i - N_j)_{\text{equilibrium}} hf_0 V}{\tau_1}. \quad (42)$$

The spin temperature  $T_x$  is conveniently related to the gain-bandwidth product if we note that  $Q_{x0}^{-1} \propto (N_i - N_j)$  and  $T_x \propto (N_i - N_j)$ . Thus,

$$T_x = \frac{|Q_{x0}|_{\text{amplification}}}{|Q_{x0}|_{\text{absorption}}} T_{\text{Lattice}}^\circ\text{K}. \quad (43)$$

<sup>14</sup> M. W. P. Strandberg, "Spin-lattice relaxation," *Phys. Rev.*, vol. 110, pp. 65-69; April 1, 1958.

where  $T_s$  is the source or antenna temperature,  $T_e$  is the cavity temperature, and  $T_0$  is the input noise temperature of the following amplifier.

For design calculations, using (25), (26), and (28), we can take

$$|Q_{x0}|_{\text{amplification}} \approx (Q_{x0})_{\text{absorption}}.$$

Thus, the curves given in Fig. 8 can be used to predict nonreciprocity, gain-bandwidth, and noise figure for the proposed amplifier.

For  $\theta = 25^\circ$ ,  $H_0 = 4.2$  kilogauss,  $T_{\text{bath}} = 4.2^\circ\text{K}$ , ruby with  $\text{Cr:Al} = 1:10^4$ ,  $B_x = 42$  mc.

$$|Q_{x0}|_{\text{amplification}+} = 210$$

$$|Q_{x0}|_{\text{amplification}-} = 1450$$

$$(Q_{x0})_{\text{pump}} = 1000$$

$$P_{\text{pump}} = 280 \mu\text{watts}$$

$$\sqrt{GB} = 42 \text{ mc}$$

Calculations of this type not only point out the way for making the best amplifier with a given system, but also clearly point out the weakness of the given system. As favorable as these figures may seem to represent our nonreciprocal ruby amplifier, they can also be used to show how unsuitable ruby is for amplifier use. The source of the disadvantage of ruby material is the anomalously low ratio of spin density to linewidth which enters in (35). Our research on the reason for this low ratio is still in progress, but preliminary results indicate that it is not attributable to the aluminum nuclear magnetic moment, nor to inhomogeneities in crystalline splitting. It is quite possible that the effect is the result of clustering of  $\text{Cr}^{+++}$  in the crystal so that the effective Cr-Cr distance is much smaller than the distance that would be computed on the basis of a random distribution of  $\text{Cr}^{+++}$  ions. In effect, this "bunching" anomalously increases the linewidth for a given concentration of  $\text{Cr}^{+++}$  over the value computed from purely random distribution of  $\text{Cr}^{+++}$  impurity ions. It has been suggested that this peaking in  $\text{Cr}^{+++}$  density distribution could arise if

the  $\text{Cr}^{+++}$  ions preferentially go into the lattice along dislocations. We cannot discuss this problem at length here, but we can say that the magnetic  $Q$  for a ruby amplifier with a  $\text{Cr}^{+++}:\text{Al}$  ratio of 1:10,000 should be five times smaller. In other words, with a ruby with a  $\text{Cr}^{+++}$  concentration of  $5:10^4$  truly randomly distributed, the magnetic  $Q$  should be approximately 40, and the line-width should still be approximately 42 mc. Notice, however, that in the equation for the gain-bandwidth product a very low magnetic  $Q$  contributes little to that product, once the latter is limited by the intrinsic paramagnetic linewidth. Thus, even with a decrease of magnetic  $Q$  factor of 5, the gain-bandwidth product increases only to 72 mc. That this is indeed the case experimentally was demonstrated by research reported previously,<sup>6</sup> which describes an experiment in which the magnitude of the magnetic  $Q$  was decreased by reducing the operating temperature from 4.2°K to 1.5°K. The measured gain-bandwidth products at these two temperatures were 43 mc and 65 mc. If the magnetic  $Q$  at 4.2°K is computed from the observed gain-bandwidth product, it will be found to be 210. The magnetic  $Q$  at 1.5°K is then 1.5/4.2 times 210, or 75, and the gain-bandwidth product computed for this magnetic  $Q$  is 62 mc, in excellent agreement with the observed value. It is for this reason that we said in the main text that gain-bandwidth products in excess of 100 mc are rather incredible unless special precautions are taken in simple regenerative cavity amplifiers, to achieve that gain-bandwidth product. Note that this result is independent of the operating frequency, and this means that the limiting gain-bandwidth product at  $L$ - or  $S$ -band would also be of the order of 50 mc.

This limitation is not widely understood. Giordmaine *et al.*<sup>15</sup> report for a single amplifier a gain-bandwidth product of 50 mc, using a permanent magnet, and 100 mc, using a laboratory magnet. No physical explanation is given, but it is implied that increase in gain-bandwidth product with the laboratory magnet was due to the greater homogeneity of the static field of the laboratory magnet. Since the magnetic  $Q$  is not the limitation here, the inverse should be true, for an inhomogeneous field will make  $B_z$  artificially larger!

It is interesting to note that, in the face of these considerations, one is not obliged to sacrifice greatly in gain-bandwidth product when operating at temperatures higher than that of liquid helium. For example, if the  $5:10^4$  ruby is operated under the conditions suggested above, a magnetic  $Q$  of approximately 40 at 4.2°K would be obtained. One can approach a temperature of 40°K by pumping on the vapor over liquid nitrogen. This means that a magnetic  $Q$  of 400 could be obtained with a liquid nitrogen refrigerant, and this would yield a gain-bandwidth product of approximately 31 mc. The

gain-bandwidth product for this same amplifier at 4.2°K would be 72. Thus, though the temperature is increased by a factor of ten, the loss in gain-bandwidth product is only 2.3.

As we have pointed out before, this limitation of gain-bandwidth product is no real limitation. Circularly-polarized cavity configuration can be conveniently cascaded because the circularly-polarized fields provide unidirectional coupling. For example, a series of three or four ruby cavities could be driven in cascade by coupling them to the circularly-polarized field which exists on the broad wall of a rectangular waveguide. Stagger-tuning the paramagnetic resonance frequencies would then give bandwidths several times  $B_z$ .

Some of the remarks made in the paper have been made rather prematurely, it is admitted, but the points are intended to be as much salutary as scientific. Only through a sure analytical understanding of the operation of these devices can the ultimate amplifier be confidently demanded, and only when it is confidently demanded will it be rapidly produced.<sup>16</sup>

#### Note:

Most of this paper was written in the Fall of 1958. The experimental results came slowly in the Spring of 1959. During this time, reports of extreme gain-bandwidth product in amplifiers constructed elsewhere—as much as 1200 mc for a single-cavity amplifier—were perplexing and indicated that our gain-bandwidth criterion<sup>1</sup> was not totally satisfactory. Paramagnetic amplifiers that we have built seem to meet our analytical expectations. Since some amplifiers that were built elsewhere apparently exceeded values allowed by the analysis herein, writing this paper made the author realize that an understanding of how to *design* such large gain-bandwidth amplifiers is obviously very important. One clue to the solution came from realizing that the reason the exponent of  $G$  in the gain-bandwidth expression is  $\frac{1}{2}$  is that the derivation essentially assumes a response of the form  $[1+x^2]^{-1}$ . With a response curve of the form  $[1+x^{2n}]^{-1}$ , the gain-bandwidth expression is  $G^{1/(2n)}B = \text{constant}$ . Thus, as  $n$  increases, *i.e.*, the response curve flattens, the bandwidth becomes increasingly independent of gain. This situation has now been resolved; and Kyhl has been able to indicate how constant-bandwidth gain-independent amplifiers can be realized with active paramagnets.<sup>12</sup> Thus, more than a year after this paper was started, although we now understand *how* larger gain-bandwidth products, using the meaningless  $\sqrt{GB}$  criterion, can occur, the implication of the paper that they must be consciously and cleverly designed for remains significant.

<sup>15</sup> J. A. Giordmaine, *et al.*, "A maser amplifier for radio astronomy at  $X$ -band," *Proc. IRE*, vol. 47, p. 1067; June, 1959.

<sup>16</sup> For a different presentation of some of these points, see P. N. Butcher, "Theory of three-level paramagnetic masers," *Proc. Inst. Elec. Engrs. (London)*, vol. 105, Part B, Supplement no. 11, pp. 684–711; May, 1958.